Inorganica Chimica Acta 362 (2009) 2872–2878

Contents lists available at ScienceDirect

Inorganica Chimica Acta

journal homepage: www.elsevier.com/locate/ica

Structure-dependent spectroscopic and redox properties of copper(I) complexes with bidentate iminopyridine ligands

Werner Massa [a], Saeed Dehghanpour [b,*], Khadijeh Jahani [b]

[a] Department of Chemistry, Philipps-University, D-35032 Marburg, Germany
[b] Department of Chemistry, Alzahra University, P.O. Box 1993891176, Tehran, Iran

ARTICLE INFO

Article history:
Received 24 September 2008
Received in revised form 29 December 2008
Accepted 9 January 2009
Available online 14 January 2009

Keywords:
Copper(I) complexes
2-Pyridinecarbaldehyde
Diimine ligands
X-ray structure analyses
Distorted tetrahedral structure
Spectroscopy

ABSTRACT

A series of iminopyridine ligands; cyclopropylpyridin-2-ylmethyleneamine (**A**), cyclopentylpyridin-2-ylmethyleneamine (**B**), cyclohexylpyridin-2-ylmethyleneamine (**C**), and cycloheptylpyridin-2-ylmethyleneamine, (**D**) and their copper(I) complexes, $[Cu(L)_2]^+$ (**1a**–**1d**) and $[Cu(L)(PPh_3)_2]^+$ (**2a**–**2d**) have been synthesized and characterized by CHN analyses, ^1H NMR and IR and UV–Vis spectroscopy. Structures of **1a**, **1b**, **1c** and **2a** were determined by X-ray crystallography. The coordination polyhedron about the Cu^I center in the complexes is best described as a distorted tetrahedron. The dihedral angles between the least-squares planes of the chelate ligands show considerable variation from 86.1° in **1a** to 68.3° in **1b**, indicating the importance of packing forces in the crystalline environment. The UV–Vis spectra of the complexes are characterized by first metal to ligand charge transfer bands increasing in wavelength with increasing size of the ring substituents in the ligands, except for the cyclopropyl compounds (**1a** and **2a**), in good agreement with the variation of the dihedral angles between the ligand planes. Cyclic voltammetry of the complexes indicates a quasireversible redox behavior for the complexes. The bulkier ligands (PPh_3) inhibit the geometric distortion within the oxidized form and the redox potentials of complexes **2a**–**2d** are shifted to more positive values, therefore.

1. Introduction

Copper(I) complexes with various *N*-donor ligands are of growing interest as most of these complexes combine remarkable features like ease of preparation, reversible electrochemical behavior, light absorption in the visible spectral region; characteristic structural flexibility, supramolecular architecture, long-lived electronically excited states, and intense luminescence [1–6]. Developments in these fields are of great interest under the point of view of various applications like solar energy conversion or catalytic activity in photo-redox reactions [7–9]. A variety of structures have been described for the Cu(I) diimine system with symmetrical and unsymmetrical chelating ligands and most of the studies have been on four-coordinated tetrahedral Cu^I complexes of the type $[Cu(NN)_2]^+$ or $[Cu(NN)(PPh_3)_2]^+$ where NN is a diimine and P is a phosphine. Factors such as the steric, electronic, and conformational interactions influence the redox potential of these complexes and modify their spectroscopic properties which are important in practical applications [10–12].

Iminopyridine ligands stabilizing low valent metal redox-states seem to be good candidates for such studies and were used for the synthesis of Cu(I), Re(I) and Ru(II) complexes in this field [13,14]. In a previous work we have studied the spectral, structural and electrochemical properties of Cu(I) complexes of phenylpyridin-2-ylmethyleneamine derivatives, but no considerable change has been observed on such properties upon variation of the ligands with different steric and electronic properties [15,16]. However, alkyl substituents in the iminopyridine ligands may modify the steric and electronic interactions and tune the physical and chemical properties of copper complexes [17–21]. To isolate the steric effect more effectively, there is clearly a need to develop iminopyridine derivatives with systematic variation of sterically active substituents in the ligands.

The following report deals with a series of diimine ligands with simple alkyl substituents where the size of an aliphatic ring varies between three and seven members. We describe the synthesis and structural characterization of Cu(I) complexes of the type $[Cu(NN)_2]^+$ and $[Cu(NN)(PR_3)_2]^+$ where NN is one of these unsymmetrical diimine ligands (**A**–**D**) (Fig. 1). We have studied the relation between the structural variation and spectroscopic changes of the complexes.

2. Experimental

2.1. General

Caution! Perchlorate salts of metal complexes with organic ligands are potentially explosive and should be handled with care.

* Corresponding author. Tel./fax: +98 021 88041344.
E-mail address: Dehganpour_farasha@yahoo.com (S. Dehghanpour).

0020-1693/$ - see front matter © 2009 Elsevier B.V. All rights reserved.
doi:10.1016/j.ica.2009.01.008

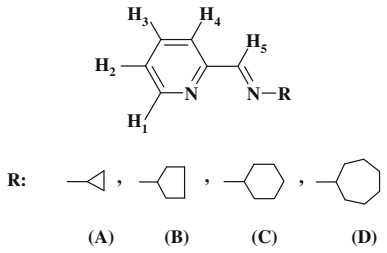

$[CuL_2]^+$		$[CuL(PPh_3)_2]^+$	
Complex	Ligand (L)	Complex	Ligand (L)
1a	A	**2a**	A
1b	B	**2b**	B
1c	C	**2c**	C
1d	D	**2d**	D

Fig. 1. Chemical formula of ligands (**A**–**D**), and Cu(I) complexes **1a**–**1d** and **2a**–**2d**.

All chemicals used were reagent grade and used as received. Solvents used for the reactions were purified by literature methods [22]. $[Cu(CH_3CN)_4]ClO_4$ and $[Cu(CH_3CN)_4]BPh_4$ were freshly prepared according to the literature procedures [23].

Elemental analyses were performed by using a Heraeus CHN-O-RAPID elemental analyzer. Infrared spectra were recorded on a Bruker Tensor 27 instrument. Electronic absorption spectra were recorded on a JASCO V-570 spectrophotometer; λ_{max} ($\log\varepsilon$). NMR spectra were obtained on a BRUKER AVANCE DRX500 (500 MHz) spectrometer. Proton chemical shifts are reported in part per million (ppm) relative to an internal standard of Me_4Si. All voltammograms were recorded with a three electrodes system consisting of an Ag/AgCl reference electrode, a platinum wire counter electrode, and Au as working electrode. A Metrohm multipurpose instrument model 693 VA processor with 694A Va stand was used. In all electrochemical experiments the test solution was purged with argon gas for at least 5 min.

2.2. Syntheses

2.2.1. Cyclopropylpyridin-2-ylmethyleneamine (*A*)

Although these types of ligands were synthesized before [24,14], here, we report a simpler method for their synthesis. To a solution of pyridine-2-carbaldehyde (107 mg, 1 mmol) in 10 ml diethylether was added a solution of cyclopropylamine (57 mg, 1 mmol) in 10 ml diethylether and stirred for 2 h. The ligand, cyclopropylpyridin-2-ylmethyleneamine was obtained as a pale yellow oil. Yield: 90%. IR, (KBr): 1628 cm^{-1} ν(C=N). ^1H NMR ($CDCl_3$, ppm): δ 0.51–0.99 (m, 4H, amine ring), 3.12 (m, 1H, amine ring), 7.18 (d, 1H, $J_{H3,4}$ = 12.84 Hz, H_4), 7.31 (dd, 1H, $J_{H3,4}$ = 9.15, $J_{H3,2}$ = 11.5 Hz, H_3), 7.76(t, 1H, $J_{H2,1}$ = 12.7, $J_{H2,3}$ = 11.35 Hz, H_2), 8.01(*d*, 1H, $J_{H1,2}$ = 7.7 Hz, H_1), 8.21(s, 1H, H_5). *Anal.* Calc. for $C_9H_{10}N_2$: C, 73.94; H, 6.89; N, 19.16. Found: C, 73.96; H, 6.89; N, 19.17%.

2.2.2. Cyclopentylpyridin-2-ylmethyleneamine (*B*)

This ligand was prepared by a procedure similar to **A** using 85 mg (1 mmol) of cyclopentylamine. Yield: 90%. IR (KBr): 1621 cm^{-1} ν(C=N). ^1H NMR ($CDCl_3$; δ): 1.40 (m, 3H, amine ring), 2.01 (m, 2H, amine ring), 3.89 (m, 1H, amine ring), 7.17 (*d*, 1H, $J_{H3,4}$ = 12.9 Hz, H_4), 7.39 (dd, 1H, $J_{H3,4}$ = 10.48, $J_{H3,2}$ = 8.8 Hz, H_3), 7.56(t, 1H, $J_{H2,1}$ = 12.6, $J_{H2,3}$ = 12.58 Hz, H_2), 7.91(d, 1H, $J_{H2,1}$ = 8 Hz, H_1), 8.17(*s*, 1H, H_5). *Anal.* Calc. for $C_{11}H_{14}N_2$: C, 75.82; H, 8.10; N, 16.08. Found: C, 75.81; H, 8.12; N, 16.9%.

2.2.3. Cyclohexylpyridin-2-ylmethyleneamine (*C*)

This ligand was prepared by a procedure similar to **A** using 99 mg (1 mmol) of cyclohexylamine. Yield: 88%. IR, (KBr): 1626 cm^{-1} ν(C=N). ^1H NMR ($CDCl_3$; δ): 0.98 (m, 1H, amine ring), 1.41 (m, 4H, amine ring), 1.81 (m, 5H, amine ring), 3.38 (m, 1H, amine ring), 7.28 (d, 1H, $J_{H3,4}$ = 12.8 Hz, H_4), 7.36 (dd, 1H, $J_{H3,4}$ = 10.85, $J_{H3,2}$ = 8.4 Hz, H_3), 7.77 (t, 1H, $J_{H2,1}$ = 12.9, $J_{H2,3}$ = 12.8 Hz, H_2), 8.12 (d, 1H, $J_{H2,1}$ = 7.4 Hz, H_1), 8.28 (s, 1H, H_5). *Anal.* Calc. for $C_{12}H_{16}N_2$: C, 75.55; H, 8.57; N, 14.88. Found: C, 75.55; H, 8.59; N, 14.87%.

2.2.4. Cycloheptylpyridin-2-ylmethyleneamine (*D*)

This ligand was prepared by a procedure similar to **A** using 113 mg (1 mmol) of cycloheptylamine. Yield: 95%. IR, (KBr): 1630 cm^{-1} ν(C=N). ^1H NMR ($CDCl_3$; δ): 1.3–1.8 (m, 12H, amine ring), 3.7 (m, 1H, amine ring), 7.25 (d, 1H, $J_{H3,4}$ = 12.8 Hz, H_4), 7.4 (dd, 1H, $J_{H3,4}$ = 8.81, $J_{H3,2}$ = 12.1 Hz, H_3), 7.74 (t, 1H, $J_{H2,1}$ = 12.4, $J_{H2,3}$ = 12.6 Hz, H_2), 7.91 (d, 1H, $J_{H2,1}$ = 7.35 Hz, H_1), 8.09 (S, 1H, H_5). *Anal.* Calc. for $C_{13}H_{18}N_2$: C, 77.18; H, 8.97; N, 13.83. Found: C, 77.16; H, 8.98; N, 13.84%.

2.2.5. $[Cu^I(A)_2]ClO_4$ (*1a*)

To a stirring solution of cyclopropylpyridin-2-ylmethyleneamine, **A** (14.6 mg, 0.1 mmol) in 5 ml acetonitrile was added $[Cu(CH_3CN)_4]ClO_4$ (16.4 mg, 0.05 mmol) in 5 ml acetonitrile and stirred for 10 min. The solution turned dark-red rapidly. The volume of the solvent was reduced under vacuum to about 4 ml. Diffusion of diethyl ether vapor into the concentrated solution gave dark-red crystals. The resulting crystals were filtered off and washed with a mixture of diethylether-acetonitrile (9:1 v/v), and dried under vacuum. Yield: 90%. IR, (KBr): 1586 cm^{-1} ν(C=N). ^1H NMR ($CDCl_3$; δ): 0.42–0.92 (m, 8H, amine ring), 3.15 (m, 2H, amine ring), 7.21 (d, 2H, $J_{H3,4}$ = 12.85 Hz, H_4), 7.33 (dd, 2H, $J_{H3,4}$ = 9.05, $J_{H3,2}$ = 11.5 Hz, H_3), 7.70(t, 2H, $J_{H2,1}$ = 12.8, $J_{H2,3}$ = 11.35 Hz, H_2), 7.92(s, 2H, H_5), 8.16(*d*, 2H, $J_{H1,2}$ = 7.7 Hz, H_1). *Anal.* Calc. for $C_{18}H_{20}ClCuN_4O_4$: C, 74.48; H, 4.43; N, 12.30. Found: C, 74.45; H, 4.45; N, 12.31%.

2.2.6. $[Cu^I(B)_2]$ BPh_4 (*1b*)

This complex was prepared by a procedure similar to **1a** using 17.4 mg (0.1 mmol) of cyclopentylpyridin-2-ylmethyleneamine, **B**. Dark-red crystals were collected by filtration and dried *in vacuo*. Yield: 93%. IR, (KBr): 1586 cm^{-1} ν(C=N). ^1H NMR ($CDCl_3$; δ): 1.45 (m, 8H, amine ring), 1.95 (m, 8H, amine ring), 3.95 (m, 2H, amine ring), 6.86(t, 4H, para H of BPh_4), 7.03 (m, 8H, meta H of BPh_4), 7.16 (*d*, 2H, $J_{H3,4}$ = 12.8 Hz, H_4), 7.43 (dd, 2H, $J_{H3,4}$ = 10.45, $J_{H3,2}$ = 8.8 Hz, H_3), 7.53(b, 8H, ortho H of BPh_4), 7.69(t, 2H, $J_{H2,1}$ = 12.8, $J_{H2,3}$ = 12.58 Hz, H_2), 7.80(*s*, 2H, H_5), 8.20(d, 2H, $J_{H2,1}$ = 8 Hz, H_1). *Anal.* Calc. for $C_{46}H_{48}BCuN_4$: C, 75.55; H, 6.62; N, 7.66. Found: C, 75.56; H, 6.61; N, 7.65%. A crystal taken for X-ray investigations before drying proved to contain one molecule of acetonitrile per formula unit.

2.2.7. $[Cu^I(C)_2]$ BPh_4 (*1c*)

This complex was prepared by a procedure similar to **1a** using 18.8 mg (0.1 mmol) of cyclohexylpyridin-2-ylmethyleneamine, **C**. Dark-red crystals were collected by filtration and dried *in vacuo*. Yield: 86%. IR, (KBr): 1585 cm^{-1} ν(C=N). ^1H NMR ($CDCl_3$; δ): 0.98 (m, 2H, amine ring), 1.30 (m, 8H, amine ring), 1.63 (m, 10H, amine ring), 3.43 (m, 2H, amine ring), 6.58 (t, 4H, Para H of BPh_4), 7.02 (m, 8H, Meta H of BPh_4), 7.27 (d, 2H, $J_{H3,4}$ = 12.75 Hz, H_4), 7.37 (dd, 2H, $J_{H3,4}$ = 10.85, $J_{H3,2}$ = 12.5 Hz, H_3), 7.52 (b, 8H, Ortho H of BPh_4), 7.74 (t, 2H, $J_{H2,1}$ = 12.85, $J_{H2,3}$ = 12.8 Hz, H_2), 7.89 (s, 2H, H_5), 8.19 (d, 2H,

$J_{H2,1}$ = 7.65 Hz, H_1). *Anal.* Calc. for $C_{48}H_{52}BCuN_4$: C, 75.93; H, 6.90; N, 7.38. Found: C, 75.95; H, 6.91; N, 7.39%.

*2.2.8. [Cu^I(D)$_2$]BPh$_4$ (**1d**)*

This complex was prepared by a procedure similar to **1a** using 20.2 mg (0.1 mmol) of cycloheptylpyridin-2-ylmethyleneamine, **D**. Dark-red crystals were collected by filtration and dried *in vacuo*. Yield: 89%. IR, (KBr): 1590 cm^{-1} ν(C=N). ^{1}H NMR ($CDCl_3$; δ): 1.28–1.75 (m, 24H, amine ring), 3.61 (m, 2H, amine ring), 6.86 (t, 4H, Para of BPh_4), 7.02 (t, 8H, Meta of Bph_4), 7.20 (d, 2H, $J_{H3,4}$ = 12.8 Hz, H_4), 7.35 (dd, 2H, $J_{H3,4}$ = 8.75, $J_{H3,2}$ = 12.1 Hz, H_3), 7.52 (b, 8H, Ortho H of BPh_4), 7.70 (t, 2H, $J_{H2,1}$ = 12, $J_{H2,3}$ = 12.65 Hz, H_2), 7.79 (S, 2H, H_5), 8.19 (d, 2H, $J_{H2,1}$ = 7.35 Hz, H_1). *Anal.* Calc. for $C_{50}H_{56}BCuN_4$: C, 76.27; H, 7.17; N, 7.12. Found: C, 76.29; H, 7.18; N, 7.11%.

*2.2.9. [Cu^I(A)(PPh$_3$)$_2$]BPh$_4$ (**2a**)*

To a 3 ml acetonitrile solution of [Cu(CH$_3$CN)$_4$]BPh$_4$ (54.8 mg, 0.1 mmol), 2 equiv. of Ph_3P (52.2 mg, 0.2 mmol) were added, and the solution was stirred for 15 min. The solvent was evaporated under vacuum at room temperature. The dry product [Cu(CH$_3$CN)$_2$(PPh$_3$)$_2$]BPh$_4$, was added to a stirring solution of 14.6 mg (0.1 mmol) cyclopropylpyridin-2-ylmethyleneamine, **A**, in 3 ml acetonitrile. The solution rapidly turned yellow, and it was stirred for 20 min at room temperature. The reaction medium was concentrated under vacuum, until the first crystals appeared in the liquid phase. Bright-yellow crystals were obtained by diffusion of diethylether vapor into the concentrated solution. Yield: 91%. IR, (KBr): 1581 cm^{-1} ν(C=N), ^{1}H NMR ($CDCl_3$; δ): 0.36 (m, 2H, amine ring), 0.78 (m, 2H, amine ring), 3.02 (m, 1H, amine ring), 6.82–7.52 (m, 53H, pyridine, Bph_4, PPh_3), 7.60 (*s*, 1H, H_5), 7.65 (d, 1H, $J_{H2,1}$ = 7.1 Hz, H_1), *Anal.* Calc. for $C_{69}H_{60}BCuN_2P_2$: C, 78.66; H, 5.74; N, 2.66. Found: C, 78.68; H, 5.75; N, 2.65%.

*2.2.10. [Cu^I(B)(PPh$_3$)$_2$]BPh$_4$ (**2b**)*

This complex was prepared by a procedure similar to **2a** using 17.4 mg (1 mmol) of cyclopentylpyridin-2-ylmethyleneamine, **B**. Bright-yellow crystals were collected by filtration and dried in *vacou*. Yield: 79%. IR, (KBr): 1583 cm^{-1} ν(C=N). ^{1}H NMR ($CDCl_3$; δ): 1.43 (m, 8H, amine ring), 3.76 (s, 1H, amine ring), 6.88–7.55 (m, 53H, pyridine, Bph_4, PPh_3), 7.75 (s, 1H, H_5), 7.83 (d, 1H, $J_{H2,1}$ = 7.2, H_1). *Anal.* Calc. for $C_{69}H_{60}BCuN_2P_2$: C, 78.66; H, 5.74; N, 2.66. Found: C, 78.68; H, 5.75; N, 2.65%.

*2.2.11. [Cu^I(C)(PPh$_3$)$_2$]BPh$_4$ (**2c**)*

This complex was prepared by a procedure similar to **2a** using 18.8 mg (0.1 mmol) of cyclohexylpyridin-2-ylmethyleneamine, **C**. Bright-yellow crystals were collected by filtration and dried in *vacou*. Yield: 90%. IR, (KBr): 1582 cm^{-1} ν(C=N).^{1}H NMR ($CDCl_3$; δ): 0.72 (m, 1H, amine ring), 1.09 (m, 4H, amine ring), 1.42 (m, 5H, amine ring), 3.25 (m, 1H, amine ring), 6.87–7.54 (m, 53H, pyridine, Bph_4, PPh_3), 7.66 (s, 1H, H_5), 7.91 (d, 1H, $J_{H2,1}$ = 6.95, H_1). *Anal.* Calc. for $C_{72}H_{66}BCuN_2P_2$: C, 78.93; H, 6.07; N, 2.56. Found: C, 78.95; H, 6.05; N, 2.57%.

*2.2.12. [Cu^I(D)(PPh$_3$)$_2$]BPh$_4$ (**2d**)*

This complex was prepared by a procedure similar to **2a** using 20.2 mg (0.1 mmol) of cycloheptylpyridin-2-ylmethyleneamine, **D**. Bright-yellow crystals were collected by filtration and dried *in vacuo*. Yield: 84%. IR, (KBr): 1582 cm^{-1} ν(C=N). ^{1}H NMR ($CDCl_3$; δ): 1.23–1.50 (m, 12H, amine ring), 3.42 (m, 1H, amine ring), 6.88–7.56 (m, 53H, pyridine, Bph_4, PPh_3), 7.67 (s, 1H, H_5), 7.92 (d, 1H, $J_{H2,1}$ = 7.45, H_1). *Anal.* Calc. for $C_{73}H_{68}BCuN_2P_2$: C, 79.01; H, 6.18; N, 2.52. Found: C, 79.02; H, 6.17; N, 2.50%.

2.3. X-ray analyses

Crystals of **1a**, **1b**, **1c** and **2a** suitable for X-ray diffraction were obtained as described above. Single crystals were mounted on Stoe IPDS area detector systems (Mo Kα λ = 0.71073 Å). The crystal data and refinement details are summarized in Table 1. The structures were solved by direct methods [25] and refined against all F^2 data using full-matrix least-squares techniques [26]. For all heavier atoms anisotropic displacement parameters were used. Though the H atoms could be located in difference Fourier maps, most of them were kept riding on idealized positions with isotropic displacement parameters taken as 1.2U_{eq} of their bonding partners. Only were significant deviations from the observed positions were found (H6, H7 in **1a**, H1a, H2a, H2b, H3a, H3b in **2a**) the positions were refined.

3. Results and discussion

3.1. Crystal structures

The crystallographic data of compounds **1a**, **1b**, **1c** and **2a** are summarized in Table 1 and selected bond distances and angles are given in Table 2.

*3.1.1. [Cu(A)$_2$]ClO$_4$ (**1a**)*

Complex **1a** crystallizes in space group *Fddd* with Z = 16. Two independent perchlorate anions are disordered on two positions with site symmetry *222* (D_2). One of them showed orientational and positional disorder. As refinements of split atom models were not very satisfying, its contribution to the diffraction data was subtracted by the back-Fourier-transform method [27]. The cation that shows C_2 symmetry is shown in Fig. 2 along with the atom-numbering scheme. While a tetrahedral geometry might be expected for a four-coordinated copper(I) center, the coordination sphere around the metal ion in this complex is distorted by the restricted bite angles of the chelating ligand. According to a bite size N1···N2 of 2.664(4) Å, the angle N2–Cu1–N1 (81.36(9)°) is much less than that in a regular tetrahedron. In contrast, the intraligand angle N2–Cu1–N2′ is much larger than 109.5°, being 134.43(15)°. The two chelate ligands that are equivalent by a 2-fold axis are almost planar (Table 3). The dihedral angle between them is with 86.1(4)° close to 90°, indicating weak sterical influence of the cyclopropyl ring.

*3.1.2. [Cu(B)$_2$]BPh$_4$ · CH$_3$CN (**1b** · CH$_3$CN)*

Compound **1b** crystallizes together with one molecule of acetonitrile in the monoclinic space group $P2_1/n$. A view of the symmetryless cation including the atom-numbering scheme is illustrated in Fig. 3.

As in complex **1a**, the coordination environment around Cu(I) of these complex is approximately tetrahedral, since the average of six angles involving Cu(I) is 110.2°. However, the coordination is clearly distorted, arising from the restricting bite angles of the chelating ligand. For **1b**, the N2–Cu1–N1 and N3–Cu1–N4 angles (81.18(5)°, 81.50(6)°) are narrower than the ideal tetrahedral angle of 109.5, whereas the opposite N2–Cu1–N4 angle (132.32(5)°) is wider (Table 2).

The five-membered rings in **1b** both show envelope conformation in different orientations. In the first ring the four atoms C10, C11, C12 and C13 are nearly planar and the atom C19 (bound to N) is at the flap by 0.615(2) Å, the folding angle at the C10···C13 axis is 143.6(1)°. In the second one, C18, C20, C21, and C22 are coplanar and C19 (not bound to N) is 0.555(2) Å above this plane, resulting in a folding angle of 140.4(2)° at the C18···C20 axis.

Table 1
Crystal data and single crystal X-ray diffraction refinement details for compounds **1a**, **1b** · CH_3CN, **1c** and **2a**.

	1a	**1b** · CH_3CN	**1c**	**2a**
Formula	$C_{18}H_{20}ClCuN_4O_4$	$C_{48}H_{51}BCuN_5$	C_{48} H_{52} B Cu N_4	$C_{69}H_{60}BCuN_2P_2$
Formula weight	455.37	772.29	759.29	1053.48
Temperature (K)	193(2)	123(2)	150(2)	193(2)
Wavelength (Å)	0.71073	0.71073	0.71073	0.71073
Crystal system	orthorhombic	monoclinic	monoclinic	monoclinic
Space group	*Fddd*	$P2_1/n$	$P2_1/n$	$C2/c$
a (Å)	13.5839(15)	10.6308(3)	27.737(3)	35.306(3)
b (Å)	24.114(2)	27.3111(8)	11.0628(6)	17.2777(15)
c (Å)	24.7107(19)	14.6340(4)	27.711(2)	18.2337(14)
α (°)	90	90	90	90
β (°)	90	109.596(2)	110.153(11)	92.885(9)
γ (°)	90	9	90	90
V (A^3)	8094.3(13)	4002.7(2)	7982.4(12)	11108.6(16)
Z	16	4	8	8
D (g cm^{-3})	1.495	1.282	1.264	1.260
μ (mm^{-1})	1.243	0.586	0.586	0.495
F(000)	3744	1632	3216	4416
Crystal size	0.50 × 0.14 × 0.03	0.46 × 0.16 × 0.13	0.55 × 0.30 × 0.30	0.50 × 0.26 × 0.20
θ Range for data collection (°)	2.36–29.26	1.65–29.18	2.37–26.80	2.24–25.88
Index ranges	$-18 \leqslant h \leqslant 18$, $-32 \leqslant k \leqslant 33$, $-32 \leqslant l \leqslant 32$	$-14 \leqslant h \leqslant 14$, $-37 \leqslant k \leqslant 36$, $-20 \leqslant l \leqslant 20$	$-35 \leqslant h \leqslant 35$, $-11 \leqslant k \leqslant 14$, $-35 \leqslant l \leqslant 35$	$-43 \leqslant h \leqslant 43$, $-21 \leqslant k \leqslant 21$, $-22 \leqslant l \leqslant 22$
Reflections collected	15677	37779	43560	47649
Independent reflections [R_{int}]	2718 [0.0763]	10785[0.0456]	16243 [0.0614]	10629 [0.0957]
Absorption correction	numerical	numerical	semi-empirical from equivalents	semi-empirical from equivalents
Maximum and minimum transmission	0.959 and 0.709	0.929 and 0.824	0.714 and 0.699	0.955 and 0.703
Refinement method	full-matrix least-squares on F^2	full-matrix least-squares on F^2	full-matrix least-squares on F^2 as $(10\bar{1})$ twin	full-matrix least-squares on F^2
Data/restraints/parameters	2718/0/134	10785/0/497	16243/0/968	10629/6/694
Goodness-of-fit on F^2	0.819	1.033	0.623	0.897
Final R indices [$I > 2\sigma(I)$]	$R_1 = 0.0430$, $wR_2 = 0.0906$	$R_1 = 0.0423$, $wR_2 = 0.0905$	$R_1 = 0.0393$, $wR_2 = 0.0518$	$R_1 = 0.0498$, $wR_2 = 0.0908$
R indices (all data)	$R_1 = 0.1076$, $wR_2 = 0.1018$	$R_1 = 0.0606$, $wR_2 = 0.0951$	$R_1 = 0.0968$, $wR_2 = 0.0572$	$R_1 = 0.1050$, $wR_2 = 0.0978$
Largest difference in peak and hole (e $Å^{-3}$)	0.334 and −0.243	0.630 and −0.305	1.072 and −0.630	0.567 and −0.417

Table 2
Selected bond lengths (Å) and bond angles (°) for **1b** · CH_3CN, **1c** and **2a**.

1a		**1b** · CH_3CN		**1c**				**2a**	
				I		II			
Cu1–N1	2.072(2)	Cu1–N1	2.0078(13)	Cu1–N1	1.943(4)	Cu2–N8	1.954(3)	Cu1–N1	2.092(3)
Cu1–N1#1	2.072(2)	Cu1–N2	2.0212(14)	Cu1–N3	2.016(3)	Cu2–N6	2.021(3)	Cu1–N2	2.104(3)
Cu1–N2	2.015(2)	Cu1–N3	2.0761(13)	Cu1–N4	2.054(4)	Cu2–N5	2.046(4)	Cu1–P1	2.2500(10)
Cu1–N2#1	2.015(2)	Cu1–N4	2.0831(14)	Cu1–N2	2.078(3)	Cu2–N7	2.079(3)	Cu1–P2	2.2521(10)
N2–Cu1–N2#1	134.43(15)	N2–Cu1–N3	129.61(6)	N1–Cu1–N3	137.34(13)	N8–Cu2–N6	137.86(13)	N1–Cu1–N2	79.12(12)
N2–Cu1–N1#1	122.33(9)	N2–Cu1–N1	81.18(5)	N1–Cu1–N4	123.86(14)	N8–Cu2–N5	124.68(15)	N1–Cu1–P2	114.21(8)
N2#1–Cu1–N1#1	81.36(9)	N3–Cu1–N1	127.93(5)	N3–Cu1–N4	80.81(15)	N6–Cu2–N5	82.40(15)	N2–Cu1–P2	109.26(8)
N2–Cu1–N1	81.36(9)	N2–Cu1–N4	132.32(5)	N1–Cu1–N2	82.60(15)	N8–Cu2–N7	82.17(14)	N1–Cu1–P1	118.78(8)
N2#1–Cu1–N1	122.33(9)	N3–Cu1–N4	81.50(6)	N3–Cu1–N2	117.27(15)	N6–Cu2–N7	113.98(14)	N2–Cu1–P1	106.35(8)
N1#1–Cu1–N1	120.46(13)	N1–Cu1–N4	108.92(5)	N4–Cu1–N2	119.63(14)	N5–Cu2–N7	119.77(14)	P2–Cu1–P1	120.04(3)
C1–N1–C5	117.2(3)	C8–N1–C1	117.68(14)	C18–N1–C19	116.9(4)	C49–N5–C53	116.3(4)	C4–N1–C1	117.8(3)
C1–N1–Cu1	131.90(19)	C8–N1–Cu1	130.36(11)	C18–N1–Cu1	111.8(3)	C49–N5–Cu2	133.3(3)	C4–N1–Cu1	112.0(2)
C5–N1–Cu1	110.83(19)	C1–N1–Cu1	110.35(10)	C19–N1–Cu1	131.1(3)	C53–N5–Cu2	110.4(3)	C1–N1–Cu1	130.2(3)
C6–N2–C7	120.1(3)	C2–N2–C9	118.27(13)	C13–N2–C17	117.8(4)	C54–N6–C55	119.4(4)	C5–N2–C9	117.4(3)
C6–N2–Cu1	112.1(2)	C2–N2–Cu1	113.68(10)	C13–N2–Cu1	132.1(3)	C54–N6–Cu2	111.3(3)	C5–N2–Cu1	112.8(3)
C7–N2–Cu1	127.6(2)	C9–N2–Cu1	128.02(11)	C17–N2–Cu1	109.8(3)	C55–N6–Cu2	128.7(3)	C9–N2–Cu1	129.6(3)

3.1.3. $[Cu(C)_2]BPh_4$ (**1c**)

Compound **1c** crystallizes in the monoclinic space group $P2_1/n$, too, with two molecules per asymmetric unit probably due to packing reasons, resulting in some small conformational differences. The crystal proved to be a pseudomerohedral $10\bar{1}$ reflection twin with a twin ratio of 60.49(5):39.51(5). Fig. 4 shows one of the cations along with the atom-numbering scheme. The spread of "tetrahedral angles" is similar to that in **1a** and **1b** (range from 80.8(2)° to 137.9(1)°, see Table 2). All four independent cyclohexyl rings in **1c** adopt an almost regular chair conformation.

3.1.4. Influence of ring size on the $[CuL_2]$ chelate complex geometry

The Cu–N bond distances (**1a** 2.044, **1b** 2.047, $\mathbf{1c_1}$ 2.028, $\mathbf{1c_2}$ 2.022 Å) are similar to that found in other pseudotetrahedral Cu(I) diimine complexes [13,28–30] (typical $Cu–N_{av}$ = 2.055 Å [30]) like the $[Cu(dpdmp)_2]^+$ cation (2.047 Å [29]). In all three compounds, the iminopyridine units are almost planar (maximum deviation from best planes 0.088 Å).

When comparing the chelate bond geometry depending on the ring substituents (Table 3), it becomes clear that the cyclopentane derivative shows the strongest distortion. In contrast to the least

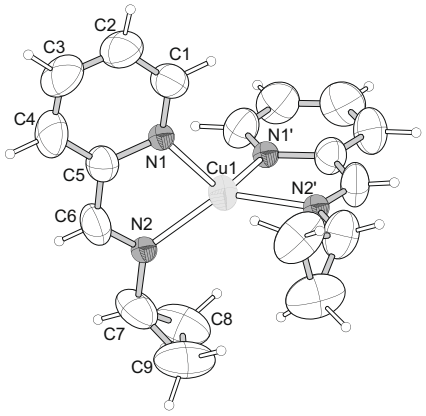

Fig. 2. Structure of the $[Cu(A)_2]^+$ cation of **1a** in the crystal, showing the atom labeling scheme. Thermal ellipsoids with 50% probability. Hydrogen atoms are omitted for clarity.

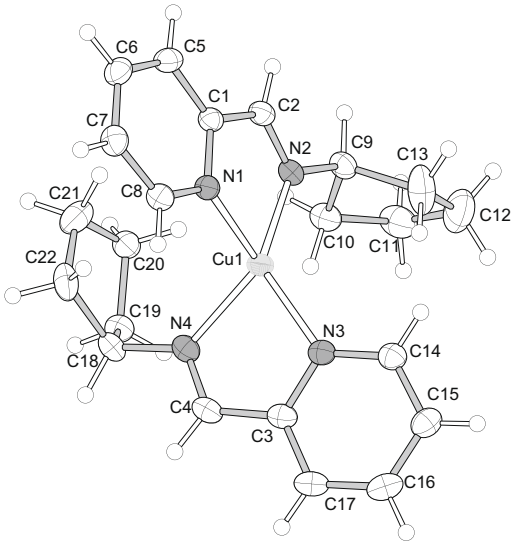

Fig. 3. Structure of the $[Cu(B)_2]^+$ cation of **1b** · CH_3CN in the crystal, showing the atom labeling scheme. Thermal ellipsoids with 50% probability. Hydrogen atoms are omitted for clarity.

distorted cyclopropane and the cyclohexane compound, the Cu atom is significantly (up to 0.32 Å) displaced out of the planes of the ligands. As well, the dihedral angle between the planes of the chelate ligands (90° in an undistorted tetrahedral complex) has a clear minimum for the cyclopentane compound **1b** (68.3°) pointing to remarkable steric interference between the bulky chelate ligands. Obviously, this effect is less for the cyclohexyl compound **1c** (dihedral angle 79.0° in average), and smallest with the cyclopropyl rest (86.1°, small distortion is also observed in **2a**, Section 3.1.5). Accordingly, the shortest contact distances between C-atoms of the ring substituents at both chelate ligands are smallest for **1b** (3.68 Å), 4.09 Å for **1a**, and 4.31/4.29 Å for **1c.** This sequence suggests that the influence of packing is crucial. The exceptional structural behavior of the cyclopropyl compound correlates with a red-shift of the first band in the optical absorption spectra as compared with the other $[CuL_2]$ complexes (vide infra).

3.1.5. *[Cu(A)(PPh$_3$)$_2$] BPh$_4$*

The cation of complex **2a**, along with the atom-numbering scheme, is shown in Fig. 5. The coordination environment around the metal ion in this complex is pseudotetrahedral with large angular distortion arising from the low intraligand N1–Cu1–N2 chelate angle, 79.12(12)°. However, the P2–Cu1–P1, 120.04(3)° angle has opened up due to the steric effects from the bulky Ph_3P ligands. The average Cu–N and Cu–P bond distances are 2.098 and 2.251 Å, respectively, and are comparable to those reported for $[Cu(dmp)(PPh_3)_2]NO_3$ (2.117(6) and 2.294(2) Å) and other copper complexes [31,32]. The dihedral angle between the best plane of the chelate ligand (N1, C4–C9, N2, maximum deviation 0.021(4) Å) and the plane defined by P1−Cu1−P2 is 88.4(5)°. However, this dihedral angle is considerably larger in comparison to the similar complexes [13,31,32]. Again, the Cu atom is displaced by 0.1374(4) Å out of the plane of the chelate ligand.

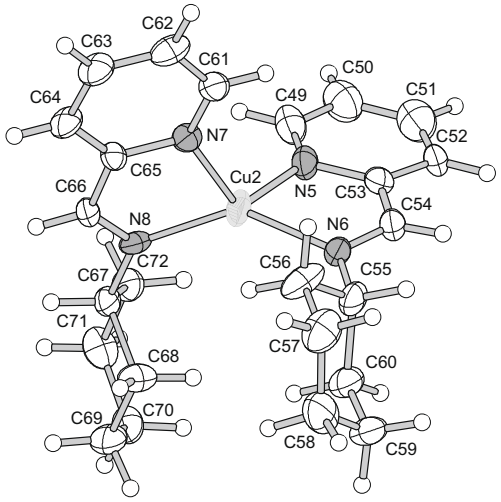

Fig. 4. Structure of the $[Cu(C)_2]^+$ cation of **1c** in the crystal, showing the atom labeling scheme. Thermal ellipsoids with 50% probability. Hydrogen atoms are omitted for clarity.

3.2. Spectroscopic characterization

The IR spectra of the free ligands exhibit ν(C=N) at 1621–1630 cm^{-1}. In complexes, ν(C=N) appears at 1581–1587 cm^{-1} and is red-shifted by 40–43 cm^{-1}. This has been attributed to the presence of d(Cu) → π^*(ligand) back bonding [33,34].

Table 3
Geometry of the $[CuL_2]$ chelate coordination in compounds **1a**, **1b** · CH_3CN, and **1c** (two independent molecules). Best planes calculated for the eight atoms of the py-CH=N-fragments.

	1a	**1b** · CH_3CN	**1c**$_1$	**1c**$_2$
Deviation (Å) from a best plane of ligand 1	0.011(4)	−0.087(1)	0.026(3)	0.074(5)
Deviation (Å) from a best plane of ligand 2	same by symmetry	−0.088(2)	0.055(4)	0.018(4)
Distance (Å) of Cu to the plane of ligand 1	0.0681(4)	−0.3162(2)	−0.1082(6)	−0.0346(6)
Distance (Å) of Cu to the plane of ligand 2		−0.1981(2)	−0.0211(6)	−0.1605(6)
Torsion angle (°) N–C=C–N (ligand 1)	1.1(5)	8.2(2)	−3.0(6)	8.2(7)
Torsion angle (°) N–C=C–N (ligand 2)		5.5(2)	−6.9(7)	2.3(6)
Dihedral angle (°) between planes 1 and 2	86.1(4)	68.31(4)	79.85(9)	78.1(1)

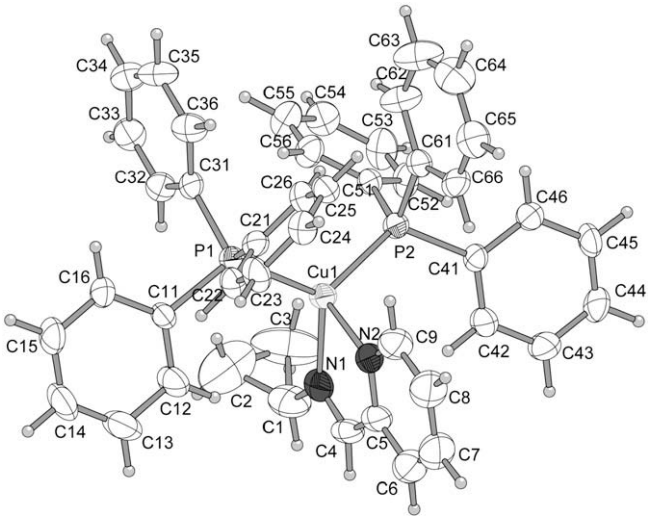

Fig. 5. Structure of the $[Cu(A)(PPh_3)_2]^+$ cation of **2a** in the crystal, showing the atom labeling scheme. Thermal ellipsoids with 50% probability.

The electronic spectra of the complexes were recorded in chloroform solution in the range 700–200 nm. The spectral data are given in Table 4. The visible range of the spectrum is dominated by a metal-to-ligand charge transfer (MLCT) transition which is a characteristic feature of copper(I) complexes when bonded to a conjugated organic chromophore [35]. The shape of the absorption spectrum of a $Cu(L)_2^+$ complex can provide some insight into the solution structure in that systems exhibiting an intense charge transfer band in the visible region [36,37]. The absorption spectrum of the $[Cu(L)_2]^+$ complexes show a band in the visible region around 470 nm. The band migrates to high wavelengths as the size of the ring substituents on the ligand increases, except for the cyclopropyl compound **1a,** the band of which appears at 483 nm. The wavelength of the first MLCT band correlates with the dihedral angle between the planes of the chelate ligands. With decreasing dihedral angle φ decreases the wavelength, for example for $\varphi = 86.1°$, $\lambda_{max} = 483$ nm in **1a**; for $\varphi = 68.31°$, $\lambda_{max} = 467$ nm in **1b** (vide supra).

$[Cu(A)(PPh_3)_2]BPh_4$ (**2a**) shows a band at 373 nm, which is shifted considerably relative to complex **1a.** A similar shift has been reported in going from $[Cu(dmp)_2]^+$ ($\lambda_{MLCT} = 454$ nm) to $[Cu(dmp)(PPh_3)_2]^+$ ($\lambda_{MLCT} = 365$ nm) [28,31,32] and also similar shifts were observed in the other $[Cu(L)(PPh_3)_2]^+$ complexes, **2b–2d** relative to the $[Cu(L)_2]^+$ complexes **1a–1d** (Table 4). An increase in the wavelength of this band is also observed with increasing of the ring size in the **2b–2d** complexes. In contrast, the higher energy band in **2a** is red-shifted and appears at 385 nm, similar to the shift observed for **1a**. Additional absorption bands are also observed in the spectra of **1a–2d** in chloroform in the UV region (Table 4). The intensities of these bands are consistent with being assigned as ligand-centered $\pi \rightarrow \pi^*$ and/or charge transfer transitions.

Table 4
IR, UV–Vis spectral data and cyclic voltammetric data of ligands and complexes.

Compound	ν(C=N) (cm^{-1})	λ_{max} (nm) (log /M^{-1} cm^{-1})	E_p^a	E_p^c
1a	1586	254 (4.45), 279 (4.25), 483 (3.49)	0.54	0.41
1b	1586	259 (4.43), 285 (4.33), 467 (3.56)	0.50	0.35
1c	1585	251 (4.31), 278 (4.39), 475 (3.47)	0.57	0.45
1d	1587	251 (4.44), 279 (4.36), 484 (3.51)	0.57	0.46
2a	1581	253 (4.19), 275 (4.33), 385 (3.45)	0.88	0.76
2b	1583	259 (4.25), 270 (4.41), 371 (3.49)	0.85	0.72
2c	1585	250 (4.30), 279 (4.39), 377 (3.44)	0.88	0.77
2d	1583	255 (4.29), 277(4.36), 381 (3.42)	0.89	0.76

The ^1H NMR spectra and peak assignments are presented in the experimental section. These peaks are assigned based on the splitting of the resonance signals, spin coupling constants and the literature, and are clearly in accordance with the molecular structure determined by X-ray crystal structure analysis. The spectra of the ligand are clearly divided into two portions; the down-field part is due to pyridine and imine protons (H_1–H_5) and the upfield signals refer to alkyl protons. Aside from the aromatic H-atoms, which appear at 7.00–8.15 ppm in the ligands, the imine protons appear as a singlet at 8.60–9.50 ppm in the ligands. The multiplet peak at about 3.7 ppm in the ligands is assigned to the proton in vicinity of imine nitrogen of the alkyl group. The other alkyl protons appear in 1–4 ppm as multiplet. The ^1H resonances of the coordinated ligands are commonly observed in complexes **1a–2d**. In complexes **2a–2d**, however, the aromatic H atoms of the coordinated Ph_3P ligands and BPh_4 anion overlap to some extent with those of the phenyl H atoms of ligands **A–D**. The down-field shift of the iminic protons in complexes relative to the free ligands can be attributed to the deshielding effect resulting from the coordination of the ligands [38,39].

3.3. Electrochemistry

The redox behavior of the complexes in CH_2Cl_2 solution was examined by cyclic voltammetry. The four ligands are electroinactive in the working potential region. The complexes (**1a–1d**) undergo a quasireversible oxidation–reduction reaction (Table 4) [40]. The response is attributed to the copper(II)/copper(I) couple ($[Cu(L)]^{2+} + e^- \; [Cu(L)]^{1+}$). The complexes show a quasireversible $Cu^{II/I}$ couple (Table 4) and the ratio of the anodic and cathodic peak currents, (i_{pa}/i_{pc}), approaches 1 as the scan rate increases. The peak-to-peak separation increases as the scan rate is changed from 50 mV/s to 500 mV/s. The $Cu^{II/I}$ potential in a Cu^IN_4 chromophore is believed to increase with increasing the electron-donating or -withdrawing properties of the ligands and the resistance to tetrahedral distortion occurring in the corresponding $Cu^{II}N_4$ chromophore [13,34]. Generally, assuming there are no extreme changes in the electron-donating or -withdrawing properties of the ligands, this redox couple can be used to indicate the resistance to tetrahedral distortion the ligands impart on the complex by observing the shift in the $Cu^{2+/+}$ redox potentials. Based on the electrochemical studies in dichloromethane (Table 4), the complexes are ranked as follows: **1b < 1a < 1c ≈ 1d**. This trend is approximately similar to the trend obtained from analysis of the absorption spectra and the dihedral angle between the planes of the chelate ligands in complexes.

An observable deviation is found for **2a–2d** where the Cu(II)/Cu(I) couple appears at a higher potential than **1a–1d.** Although a higher degree of conjugation exists in **1a–1d** relative to **2a–2d**, the existence of bulkier ligands in **2a–2d** which prevent the inner-sphere reorganization to flattened tetrahedral, more appropriate to Cu(II) oxidation state, play a key role in shifting the oxidation potential to higher values for complexes **2a–2d** relative to **1a–1d**.

4. Conclusion

A series of $[Cu(L)_2]^+$ and $[Cu(L)(PPh_3)_2]^+$ complexes with systematic variation of aliphatic rings in iminopyridine ligands L has been synthesized for examining the influence of structural variation on the spectroscopic and redox properties of the complexes. Structural studies show less distorted geometries in the cyclopropyl compounds, most distortion at the cyclopentyl derivative. Comparison of the series of $[Cu(L)_2]^+$ complexes shows a clear correlation between geometric distortion upon variation of the ligands and the spectroscopic and redox properties. Red shift of

the MLCT absorption band is observed when the dihedral angle between the best planes of the chelate ligand increases. Our results indicate that the position of the MLCT band changes considerably and is blue shifted when one of the iminopyridine ligands is replaced by two Ph_3P molecules. The additional steric hindrance in complexes of $[Cu(L)(PPh_3)_2]^+$ relative to $[Cu(L)_2]^+$ results in a more positive $Cu^{II/I}$ redox potential.

5. Supplementary material

CCDC 701942, 701943, 701945, and 701944 contain the supplementary crystallographic data for compounds **1a**, **1b**, **1c**, and **2a**, respectively. These data can be obtained free of charge from The Cambridge Crystallographic Data Centre via www.ccdc.cam.ac.uk/data_request/cif.

References

[1] C.T. Cunningham, K.L.H. Cunningham, J.F. Michalec, D.R. McMillin, Inorg. Chem. 38 (1999) 4388.
[2] D.R. McMillan, J.R. Kirchhoff, K.V. Goodwin, Coord. Chem. Rev. 64 (1985) 83.
[3] B.G. Malmstrom, in: R.J.P. Williams, J.R.R.F. De Silva (Eds.), New Trends in Bioinorganic Chemistry, Academic Press, New York, 1978, p. 59.
[4] N. Armaroli, Chem. Soc. Rev. 30 (2001) 113.
[5] G.A. Hogan, A.A. Gallo, K.M. Nicholas, R.S. Srivastava, Tetrahedron Lett. 43 (2002) 9505.
[6] S. Mahadevan, M. Palaniandavar, Inorg. Chem. 37 (1998) 693.
[7] F. Liu, K.A. Meadows, D.R. McMillin, J. Am. Chem. Soc. 115 (1993) 6699.
[8] M. Ruthkosky, C.A. Kelly, F.N. Castellano, G.J. Meyer, Coord. Chem. Rev. 171 (1998) 309.
[9] S. Sakaki, T. Kuroki, T. Hamada, J. Chem. Soc., Dalton Trans. 840 (2002).
[10] D.V. Scaltrito, D.W. Thompson, J.A. O'Callghan, G.J. Meyer, Coord. Chem. Rev. 208 (2008) 243.
[11] A.Y. Kovalevsky, M. Gembicky, I.V. Novozhilova, P. Coppens, Inorg. Chem. 42 (2003) 8794.
[12] M. Ruthkosky, C.A. Kelly, M.C. Zaros, G.J. Meyer, J. Am. Chem. Soc. 119 (1997) 12004.
[13] S. Goswami, W. Kharmawphlang, A.K. Deb, S.M. Peng, Polyhedron 20 (1996) 3635.
[14] R.N. Dominey, B. Hauser, J. Hubbard, J. Dunham, Inorg. Chem. 30 (1991) 4754.
[15] S. Dehghanpour, N. Bouslimani, R. Welter, F. Mojahed, Polyhedron 26 (2007) 154.
[16] S. Dehghanpour, A. Mahmoudi, Main Group Chem. 6 (2007) 121.
[17] R.M. Everly, D.R. McMillin, J. Phys. Chem. 95 (1991) 9071.
[18] M.T. Miller, P.K. Gantzel, T.B. Karpishin, Inorg. Chem. 38 (1999) 3414.
[19] V. Desvergnes-Breuil, V. Hebbe, C. Dietrich-Buchecker, J-P. Sauvage, J. Lacour, Inorg. Chem. 42 (2003) 255.
[20] G.C. Van Stein, G. van koten, B. Debok, L.C. Taylor, K. Vrieze, C. Brevard, Inorg. Chim. Acta 89 (1984) 29.
[21] A.K. Ichinaga, J.R. Kirchhoff, D.R. McMillin, C.O. Dietrich-Buchecker, P.A. Marnot, J.-P. Sauvage, Inorg. Chem. 26 (1987) 4290.
[22] D.D. Perrin, W.L. Armarego, D.R. Perrin, Purification of Laboratory Chemicals, 2nd ed., Pergamon, New York, 1990.
[23] P. Hemmerich, C. Sigwart, Experientia 488 (1963) 15.IX.
[24] E.V. Dose, L.J. Wilson, Inorg. Chem. 2660 (1978) 17.
[25] G.M. Sheldrick, SHELXS97, Program for the Solution of Crystal Structures, Universität Göttingen, 1997.
[26] G.M. Sheldrick, SHELXL97, Program for the Refinement of Crystal Structures, Universität Göttingen, 1997.
[27] P.V.D. Sluis, A.L. Spek, Acta Crystallogr. A 46 (1990) 194.
[28] R. Hadjikhani, S. Dehghanpour, A. Mahmoudi, F. Mojahed, Z. Anorg. Allg. Chem. 723 (2006) 632.
[29] C.T. Cunnighum, J.J. Moore, K.L.H. Cunningham, P.E. Fanwick, D.R. McMillin, Inorg. Chem. 39 (2000) 3638.
[30] S. Dehghanpour, L. Fotouhi, M.M. Amini, H.R. Khavasi, K. Jahani, F. Nouroozi, E. Zamanifar, J. Coord. Chem. 61 (2008) 455.
[31] J.R. Kirchhoff, D.R. McMillin, W.R. Robinson, D.R. Powell, A.T. McKenzie, S. Chen, Inorg. Chem. 24 (1985) 3928.
[32] R.A. Rader, D.R. McMillin, M.T. Buckner, T.G. Matthews, D.J. Casadonte, R.K. Lengel, S.B. Whittaker, L.M. Darmon, F.E. Lytle, J. Am. Chem. Soc. 103 (1981) 5906.
[33] K. Nakamoto, Infrared and Raman Spectra of Inorganic and Coordination Complexes, 4th ed., John Wiley & Sons, USA, 1992.
[34] M. Amirnasr, G. Kickelbick, S. Dehghanpour, Helv. Chim. Acta 89 (2006) 274.
[35] S. Sakaki, H. Mizutanti, Y. Kase, Inorg. Chem. 31 (1992) 4375.
[36] P.J. Burke, D.R. McMillin, W.R. Robinson, Inorg. Chem. 19 (1980) 1211.
[37] K. Shinozaki, Y. Kaizu, Bull. Chem. Soc. Jpn. 67 (1994) 2435.
[38] M. Ruthkosky, F.N. Castellano, G.J. Meyer, Inorg. Chem. 35 (1996) 6406.
[39] M.K. Eggleston, D.R. McMillin, K.S. Koenig, J.A. Pallenberg, Inorg. Chem. 36 (1997) 172.
[40] A.J. Bard, L.R. Faulkner, Electrochemical Methods, Fundamentals and Applications, John Wiley & Sons, New York, 1980.